Odd characteristics of Au film on pentacene

Kyuwook Ihm
Department of Physics, Pohang University of Science and Technology, Pohang 790-784, Korea and Pohang Accelerator Laboratory, Pohang University of Science and Technology, Pohang 790-784, Korea

Hye-Eun Heo and Sukmin Chung[a)]
Department of Physics, Pohang University of Science and Technology, Pohang 790-784, Korea

Joung-Real Ahn
BK21 Physics Research Division, Sungkyunkwan University, Suwon 440-746, Korea and SKKU Advanced Institute of Nano Technology (SAINT), Sungkyunkwan University, Suwon 440-746, Korea

Jung Hyun Kim
Department of Mechanical Engineering, Korea Advanced Institute of Science and Technology (KAIST), Daejeon 305-701, Korea

Tai-Hee Kang
Pohang Accelerator Laboratory, Pohang University of Science and Technology, Pohang 790-784, Korea

(Received 19 April 2007; accepted 21 May 2007; published online 14 June 2007)

Anomalies of Au film formed on the pentacene surface are investigated as a counterpart of pentacene/Au structure. The Au film is found to contain pentacene derivatives originated from the pentacene layers, and it is composed of grains of various sizes formed as the Au thickness increases. The authors suggest that it is this abundance of peculiarities of the Au film that accounts for the attenuated density of states in the valence band. Deformation of Au grains is accompanied by the lift of the pentacene layers, which, in turn, brings about the device failure. © *2007 American Institute of Physics*. [DOI: 10.1063/1.2748334]

Substantial progress has been made in electronic devices based on organic semiconductors, and this has motivated a renewal of fundamental research on key factors governing the device performance.[1–4] The Au/pentacene interface has been attracting attention because it differs in electrical behavior from the pentacene/Au interface.[4–9] The asymmetric nature of metal/organic and organic/metal structures has been utilized in developing the memory device.[8] A number of studies have been conducted on the interesting adsorption mechanism of the organic molecules on the metal. As a result much detailed information is available on the pentacene/Au interface.[10,11] In the case of the Au/pentacene interface, however, only a few phenomena have been reported such as diffusion of Au into the pentacene layers, unexpected carbon atoms on the Au film, and variation of device performance depending on the Au deposition conditions.[5,6]

This letter shows that the electronic structures near the Fermi level of the Au/pentacene surface are different from those of the Au/SiO_x surface. We confirmed that anomalies in the electronic structures of the Au/pentacene surface are caused by the unexpected carbon atoms and irregular morphologies concurrently observed in the Au film. The origin of the carbon species is investigated using synchrotron radiation spectroscopy and calculations based on Fick's second law. The microscopic analysis shows that the Au film at various thicknesses has different morphologies resulting from the relaxation of the intergranular, interlayer stresses and thermal contraction during the process of cooling down the sample after Au deposition. The deformation of the Au grains resulting from the relaxation of stresses lifts the pentacene layers from beneath the Au film.

The sample preparations and spectroscopic measurements were carried out at 4B1 Beamline of Pohang Accelerator Laboratory in Korea.[12] The flux of the thermally evaporated pentacene molecules and Au atoms was controlled to be 0.2 Å/s by using the thickness monitor. The valence band spectra and the secondary cutoff were acquired by the ultraviolet source (Omicron, He I line). Near edge x-ray absorption fine structure (NEXAFS) measurements in partial electron yield mode were performed by counting the carbon *KLL* Auger electrons. The unloaded samples were characterized by scanning electron microscopy (SEM) (JEOL JSM-7401F), atomic force microscopy (AFM) (PSIA XE-100), and transmission electron microscopy (TEM) (JEOL JEM-3011).

Figure 1(a) shows the valence band spectra from the Au film on the SiO_x and the pentacene surfaces. All the spectra were normalized to equalize the intensity at 9 eV. The overall spectrum of the Au/SiO_x surface is very similar to that of the Au (111) surface.[13] The features marked by B_1, B_2, and B_3 stand for the upper Au $5d$ bulk bands, and S_1 and S_2 are surface states.[13] In the spectrum of the Au 4 Å/pentacene surface, broad features originated from the Au film begin to appear. Although Au is sufficiently thicker than the photoelectron spectroscopy probing depth, no prominent peak development is observed in the spectrum of the Au 600 Å/pentacene surface. Because of such broadness and low intensity of the spectral features, it is hard to discern the detailed peaks. These broad features are related to the density of defects and mixed surfaces that have different surface indices. Figure 1(b) shows the work function shifts recorded

a)Author to whom correspondence should be addressed; electronic mail: smc@postech.ac.kr

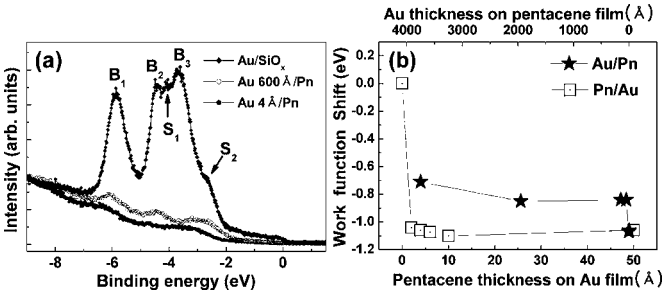

FIG. 1. (a) Valence band spectra from the Au 200 Å/SiO_x (filled diamonds), Au 600 Å/pentacene 200 Å/SiO_x (empty circles), and Au 4 Å/pentacene 200 Å/SiO_x (filled circles) surfaces. (b) Plots of the work function changes with respect to that of the clean Au(111) surface. Empty squares represent measured values on the pentacene/Au surface as the pentacene thickness was varied along the lower x axis. Filled stars represent measured values on the Au/pentacene/SiO_x surface as the Au thickness was varied along the upper x axis.

on the pentacene/Au surface as the thickness of pentacene increases and those recorded on the Au/pentacene/SiO_x surface as the thickness of Au increases. At the initial stage of pentacene deposition on the Au surface, the work function was abruptly lowered by approximately 1.1 eV and became saturated after 5 Å. In Fig. 1(b), the work function changes in the reversed structure are represented by filled stars. Although the Au thickness on the pentacene surface reaches 3800 Å, the work function of the Au film does not return to zero. Instead, it records 0.7 eV, which is lower than that of the pure Au film. These results agree with the previous research.[9]

To explore the origins of the asymmetric behavior, the Au film on the pentacene surface was carefully reinvestigated as a function of the Au thickness by using the spectroscopic and microscopic methods. As mentioned above, the valence band spectra of the Au/pentacene surface indicated the presence of the high density of defects. Park *et al.* have reported the unexpected carbon on the Au film whose origin was unclear.[6]

Figure 2(a) shows the NEXAFS spectra of the pentacene 200 Å/SiO_x and Au 200 Å/pentacene 200 Å/SiO_x surfaces. In the spectrum of the Au/pentacene/SiO_x surface, the sharp feature at 286 eV and the broad features in the region of 290–315 eV coincide with the π^* resonance peak excited from the C 1s level to LUMO+1 (lowest unoccupied molecular orbital) and also with the σ^* resonances in the pentacene film.[14] One difference is the disappearance of the peak

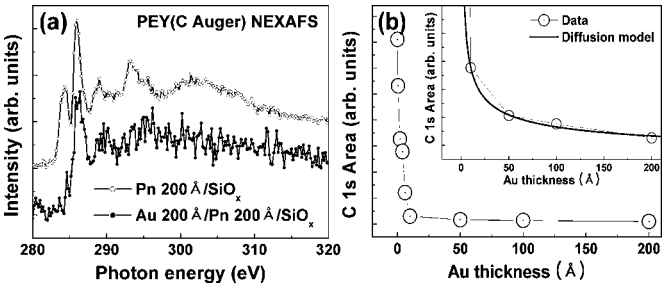

FIG. 2. (a) NEXAFS spectra at 45° of incident angle using p-polarized photons around carbon K edge from the pentacene 200 Å/SiO_x and Au 200 Å/pentacene 200 Å/SiO_x surfaces. (b) Plots of C 1 s intensity using 430 eV of photons. The inset shows experimental plots and the best fitted curve by a density function solved from Fick's second law when $D=2.16\times10^{-15}$ cm^2/s.

at 284 eV attributed to the excitation from the C 1s level to LUMO. The LUMO has been reported to be localized at outer carbon atoms that compose the pentacene molecule. This means that the resonance peak at 284 eV is easily affected by foreign species generated during chemical reactions.[5,14] This also means that the disappearance of the peak is attributed to the affluent Au atoms that surround the pentacene molecules on the surface.[15] These results indicate that the unexpected carbon atoms on the Au/pentacene/SiO_x surface are originated from the pentacene layers beneath the Au film rather than from external sources.

The most probable origin of the pentacene derivatives in the Au film is readsorption of the pentacene molecules in the gas phase around the sample induced by the hot Au atoms while exposing the pentacene surface to the Au flux. This suggestion is supported by the fact that the pentacene molecules desorb above 340 K and that the temperature of the pentacene/ SiO_x sample reached up to 360 K during Au evaporation.[16,17] However, the outdiffusion of the pentacene molecules through the imperfect Au film is another pathway that needs to be considered. To test the possibility of the outdiffusion, the behavior of the C 1s level intensity on the varied thickness of the Au film was compared with the calculated value by using the redistribution diffusion model based on Fick's second law, in which the carbon concentration at Z (Au thickness)=0 decreases as diffusion time increases.[18] The intensity of the C 1s level can be expressed as

$$I_c \propto n_c(\lambda - Z) + \int n_c^d dZ, \tag{1}$$

where n_c is the density of carbon in the pentacene layers, n_c^d is the density of diffused carbon in the Au bulk, and λ is the electron mean free path. For $Z<\lambda$, I_c is dominated by the first term in Eq. (1). The first term goes to zero when Z approaches λ, which corresponds to the initial steep slope in Fig. 2(b) and reveals $\lambda \approx 10$ Å. For $Z>\lambda$, I_c is described by the second term in Eq. (1) as

$$I_c \propto \int_{Z-\lambda}^{Z} n_c^d(Z,t)dZ. \tag{2}$$

The solution of the redistribution diffusion model based on Fick's second law is given by $n_c^d(Z,t)=(Q_0/\sqrt{\pi Dt})\exp(-Z^2/4Dt)$, where D is the diffusion coefficient and Q_0 (at./cm^3) is the total dose.[18] Because the diffusion process is most activated during Au evaporation when the sample temperature is elevated up to 360 K, the diffusion time was estimated by dividing the Au thickness by the Au flux. Then, by using $t=Z/(0.2\ \text{A/s})$ and $n_c^d(Z,t)\approx n_c^d(Z-\lambda,t)$, Eq. (2) gives $I_c \propto (1/\sqrt{Z})\exp(-Z/20D)$. This equation was used to fit the experimental data as depicted in the inset of Fig. 2(b), in which the solid curve is obtained when D is 2.16 $\times10^{-15}$ cm^2/s. This value is unreasonably high because it is close to that of a single carbon atom in the iron bulk.[19] These results show that outdiffusion is not a major mechanism which brings pentacene molecules to the Au surface.

Figure 3 shows the images photographed by using the SEM, AFM, and TEM. The SEM images indicate that the morphology depends on the thickness of the Au film on the pentacene surface. Uniform surface images are observed at 300 and 400 Å of Au, whereas coarse surface images are

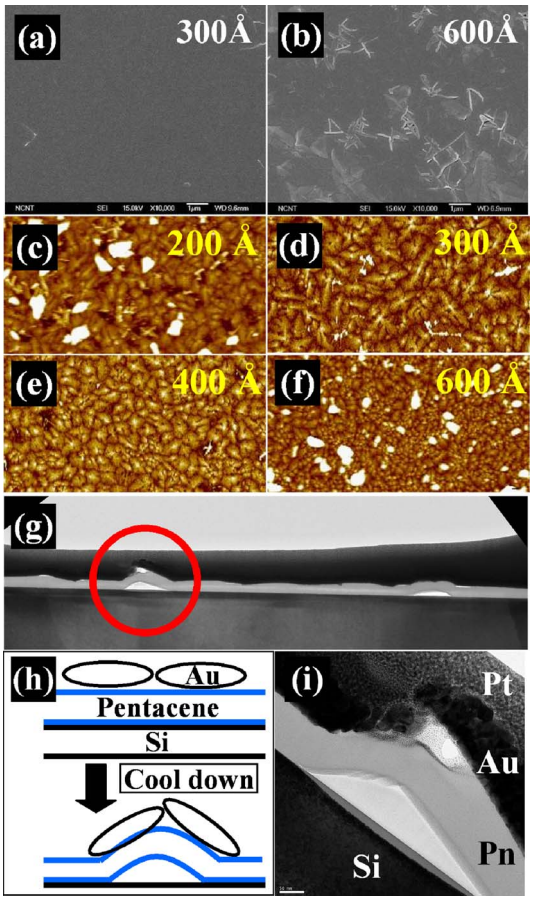

FIG. 3. (Color online) SEM images on the (a) Au 300 Å/pentacene/SiO_x and (b) Au 600 Å/pentacene/SiO_x surfaces. AFM images (10×20 μm^2) with a higher depth resolution on the (c) Au 200 Å/pentacene/SiO_x, (d) Au 300 Å/pentacene/SiO_x, (e) Au 400 Å/pentacene/SiO_x, and (f) Au 600 Å/pentacene/SiO_x surfaces. High resolution TEM images taken on the cross section of the Pt/Au 600 Å/pentacene 800 Å/SiO_x sample show the deformation of the (g) Au and pentacene layers. Pt is deposited on the sample for avoiding the charging effect of the sample during taking the TEM image. (i) shows the enlarged image of the marked area by circle in (g). (h) shows schematic view of the deformation process of the Au film.

observed at 200 and 600 Å. Figures 3(a) and 3(b) show the best and the worst surface images at 300 and 600 Å, respectively. The AFM image taken from the Au 300 Å/pentacene surface clearly shows the distribution of grains, while the uniform surface is observed by the SEM. The grains and defects in the surface indicate mixed surfaces with different surface indices as well as uneven height, which explains why the features in the valence band spectra from the Au film on the pentacene surface are broader than those of the Au crystal.[13] The protrusions shown in (c) and (f) correspond to the disordered defects in (b). The cross section of the protrusion on the Au 600 Å/pentacene surface is shown in Fig. 3(g) by utilizing the TEM. In Fig. 3(g), a feature marked by a circle shows the lift of the pentacene layers that resulted from the deformation of Au grains. As the thickness of the Au film increases, the intrinsic and external stresses accumulate. When the sample starts to cool down after the Au evaporation, a thermal stress is produced from the different coefficients of thermal expansion between the Au film and pentacene. A relaxation of the accumulated stresses induces deformation, as depicted in Fig. 3(h). This is an example of the device failure that occurs due to the preparation method of the metal contact. Accordingly, the molecular devices composed of only several molecular layers are expected to be more susceptible to failure.

In summary, pentacene derivatives are observed in the Au film on the pentacene surface. The spectroscopic results and the calculations based on Fick's second law indicate that the major origin of the pentacene derivatives is readsorption of the desorbed pentacene molecules caused by hot Au atoms. A microscopic analysis showed that the deformation of the Au grains is caused by the relaxation of accumulated stresses that accompanies the lift of the pentacene layers beneath the Au film. Pentacene derivatives and coarse morphologies observed on the Au film are suggested as causes of valence band broadening.

This work was supported partly by the Korea Research Foundation Grant funded by the Korean Government (MOE-HRD) KRF-2006-311-C00307 and KRF-2005-005-J11903.

[1]W. F. Aerts, S. Verlaak, and P. Heremans, IEEE Trans. Electron Devices **49**, 2124 (2002).
[2]H. Klauk, M. Halik, U. Zschieschang, C. Schmid, and W. Radlik, J. Appl. Phys. **92**, 5259 (2002).
[3]J. Xue and S. R. Forrest, Appl. Phys. Lett. **82**, 136 (2003).
[4]M. Halik, H. Klauk, U. Zschieschang, G. Schmid, C. Dehm, M. Schütz, S. Maisch, F. Effenberger, M. Brunbauer, and R. Stellacci, Nature (London) **431**, 963 (2004).
[5]J. H. Cho, D. H. Kim, Y. Jang, W. H. Lee, K. Ihm, J.-H. Han, S. Chung, and K. Cho, Appl. Phys. Lett. **89**, 132101 (2006).
[6]J. Park, S. I. Kang, S. P. Jang, and J. S. Choi, Jpn. J. Appl. Phys., Part 1 **44**, 648 (2005).
[7]F.-J. Meyer zu Heringdorf, M. C. Reuter, and R. M. Tromp, Nature (London) **412**, 517 (2001).
[8]D. Tondelier, K. Lmimouni, D. Vuillaume, C. Fery, and G. Haas, Appl. Phys. Lett. **85**, 5763 (2004).
[9]N. J. Watkins, L. Yan, and Y. Gao, Appl. Phys. Lett. **80**, 4384 (2002).
[10]K. Ihm, B. Kim, T. H. Kang, K. J. Kim, M. H. Joo, T. H. Kim, S. S. Yoon, and S. Chung, Appl. Phys. Lett. **89**, 033504 (2006).
[11]J. H. Kang and X.-Y. Zhu, Appl. Phys. Lett. **82**, 3248 (2003).
[12]T-H. Kang, Ki-Jeong Kim, C. C. Hwang, S. Rah, C. Y. Park, and B. Kim, Nucl. Instrum. Methods Phys. Res. A **467-468**, 581 (2001).
[13]H.-G. Zimmer, A. Goldmann, and R. Courths, Surf. Sci. **176**, 115 (1986).
[14]M. Alagia, C. Baldacchini, M. G. Betti, F. Bussolotti, V. Carravetta, U. Ekström, C. Mariani, and S. Stranges, J. Chem. Phys. **122**, 124305 (2005).
[15]J. Repp, G. Meyer, S. Paavilainen, F. E. Olsson, and M. Persson, Science **312**, 1196 (2006).
[16]G. Hughes, J. Roche, D. Carty, T. Cafolla, and K. E. Smith, J. Vac. Sci. Technol. B **20**, 1620 (2002).
[17]D. Guo, S. Ikeda, K. Saiki, H. Miyazoe, and K. Terashima, J. Appl. Phys. **99**, 094502 (2006).
[18]S. Wolf and R. N. Tauber, *Silicon Processing for the VLSI Era*, 2nd ed. (Lattice, Sunset Beach, CA, 2000), Vol. 1, p. 242.
[19]C. Kittel, *Introduction to Solid State Physics*, 7th ed. (Wiley, New York, 1960), Vol. 1, p. 544.